A&A 366, 891–897 (2001)
DOI: 10.1051/0004-6361:20000259

Astronomy & Astrophysics

Detection of optical oscillations of the intermediate polar V709 Cassiopeae (RX J0028.8+5917)

V. P. Kozhevnikov

Astronomical Observatory, Ural State University, Lenin Av. 51, Ekaterinburg, 620083, Russia

Received 4 August 2000 / Accepted 8 November 2000

Abstract. We report detection of low-amplitude optical oscillations at periods of 312.77 s and 317.94 s of the intermediate polar V709 Cas. Within the accuracy of measurement these periods agree with the X-ray period reported by Motch et al. (1996) and refined by Norton et al. (1999) and its synodic counterpart if we specify an orbital period of 5.4 h, which is one of the two possible orbital periods reported by Motch et al. (1996). The oscillation at a period of 317.94 s has the strong first harmonic which is evidence for the nonsinusoidal pulse profile of this oscillation. The data folded at a period of 317.94 s reveal a double-peaked pulse profile of this oscillation, which is highly variable from night to night. A weak periodic signal corresponding to the first harmonic of the oscillation at a period of 312.77 s is also detected in the lightcurves of V709 Cas.

Key words. stars: individual: V709 Cas – stars: novae, cataclysmic variables – stars: oscillations

1. Introduction

Intermediate polars form a subgroup of cataclysmic variables having a magnetized white dwarf which accretes the matter from its late type companion. The rotation of the white dwarf is not phase-locked to the binary period of the system. An offset between the rotation axis and the magnetic dipole axis of the white dwarf causes oscillations in the X-ray and optical wavelength bands. The X-ray pulsation period is usually identified as the spin period of the white dwarf. In addition to spin and orbital periods, the reprocessing of X-rays at some part of the system that revolves at the binary period gives rise to emission that varies with the beat period, where $1/P_{\rm beat} = 1/P_{\rm spin} - 1/P_{\rm orbit}$. This synodic counterpart is often called the orbital sideband of the spin frequency. A comprehensive review of intermediate polars is given by Patterson (1994).

The source RX J0028.8+5917 was recognized as an intermediate polar by Haberl & Motch (1995), following its detection in the ROSAT All Sky Survey. A follow up pointed observation revealed a pulse period of 312.8 s. Motch et al. (1996) identified the X-ray source with a 14th magnitude blue star, V709 Cas. The optical spectra of this star show radial velocity variations with periods of either 5.4 h or 4.45 h. One of these periods is assumed to be the orbital period of the system. However, the CCD photometric observations made by Motch et al. (1996) did not reveal optical oscillations at the X-ray period due probably to insufficient time resolution of the CCD system. In order to detect optical oscillations at or near the X-ray pulsation period and to search for other periodicities in the system, we conducted high-speed photometric observations of V709 Cas on six consecutive nights in October 1999. In this paper we present results from all our observations, spanning a total duration of 42 hours.

Send offprint requests to: V. P. Kozhevnikov,
e-mail: valerij.kozhevnikov@usu.ru

2. Observations and analysis

V709 Cas was observed on 1999 October 4–9, using a three-channel (two stars + sky) photometer attached to the 70 cm telescope at Kourovka Observatory of the Ural State University. A journal of the observations is given in Table 1. The program and nearby comparison stars were observed through 16″ diaphragms in the first and second channels, and the sky background was observed in the third channel. Data were collected at 8 s sampling times in white light (approximately 3000–7000 Å), employing a PC based data acquisition system. The design of the photometer is described by Kozhevnikov & Zakharova (2000). The continuous measurements of the sky background were subtracted from the program and comparison star data, taking into account the differences in light sensitivity between the channels. Then we took differences of magnitudes of the program and comparison stars. Because the angular separation between the program and comparison stars is only a few arcminutes, the differential magnitudes are corrected for first order atmospheric extinction and

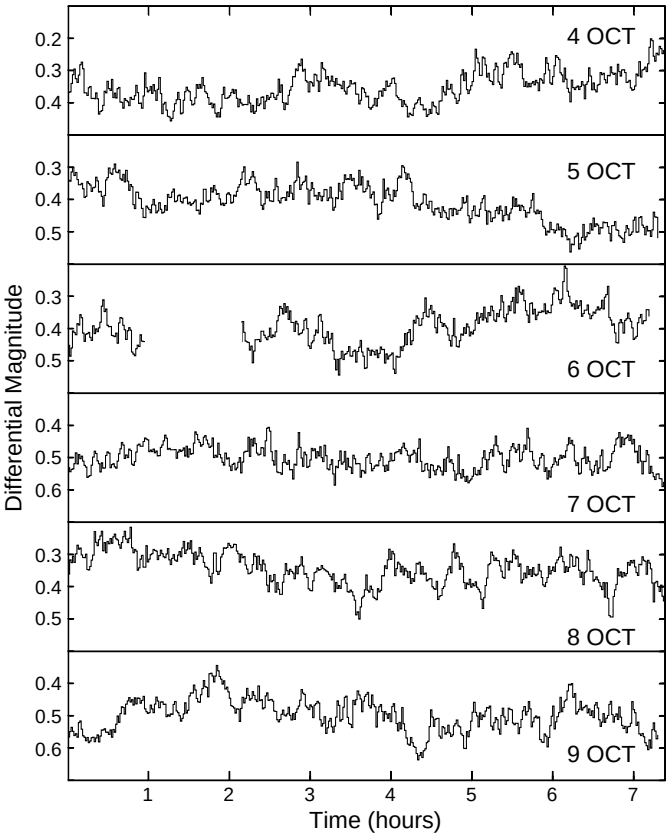

Fig. 1. Differential lightcurves of V709 Cas. The magnitudes are averaged over 64 s time intervals, and the mean rms noise of the lightcurves equals 0.009 mag

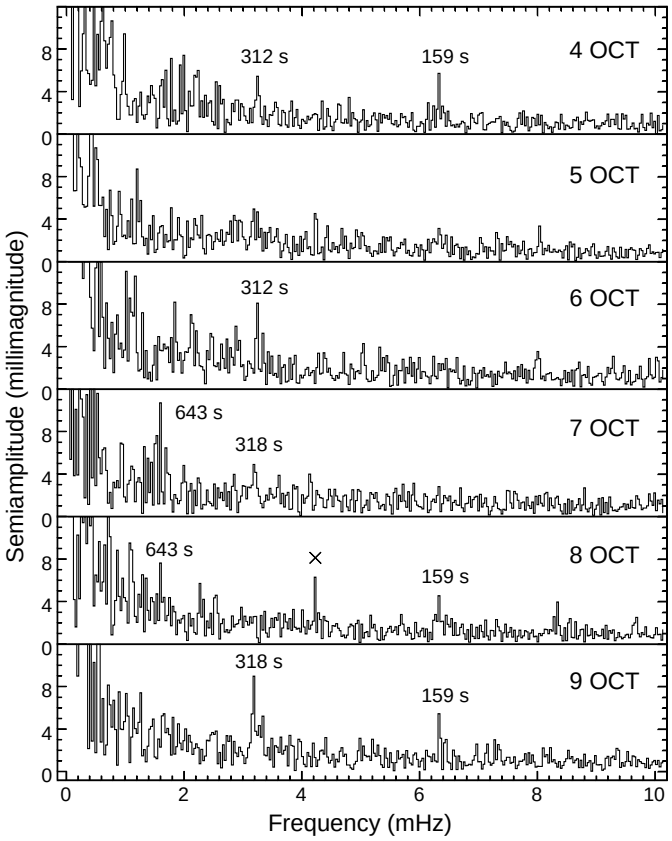

Fig. 2. Amplitude spectra of V709 Cas. Prominent peaks are labeled with their periods in seconds. The peak marked with cross is an artifact caused by the telescope drive error

light absorption by thin clouds appeared sometimes during the observations.

The mean counts are 8300, 9700 and 2500 for V709 Cas, the comparison star and the sky background in the first and second channels, accordingly. These counts result in the photon noise (rms) of the differential lightcurves, which is equal to 0.023 mag. The sky background measured through a diaphragm of about 30″ in the third channel is about 10 000 and cannot produce appreciable additional noise after its subtraction from the program and comparison star data since this sky background is corrected for the differences in light sensitivity between the channels. After this correction the variance of this sky background is smaller by a factor of about 4 in comparison with the variance of the sky background in the first and second channels. The actual rms noise of the differential lightcurves includes also the noises due to atmospheric scintillations and motion of the star images in the diaphragms. We estimate these noises roughly equal to 0.005 mag each. The actual rms noise of the differential lightcurves is somewhat larger than the photon noise and approximately equal to 0.024 mag. It is not possible to show our long lightcurves of V709 Cas with a time resolution of 8 s graphically. Figure 1 presents the differential magnitudes averaged over 64 s time intervals. The rms noise of these lightcurves is smaller by a factor of $\sqrt{8}$ and equal to 0.009 mag. A detailed description of the noise analysis carried out for the photometer is given by Kozhevnikov & Zakharova (2000).

Table 1. Journal of the observations

date (UT)	HJD start (−2 451 400)	length (hours)
1999 Oct. 4	56.41120	7.37
1999 Oct. 5	57.41177	7.30
1999 Oct. 6	58.41418	7.20
1999 Oct. 7	59.39877	7.37
1999 Oct. 8	60.39690	7.37
1999 Oct. 9	61.40149	7.30

3. Results and discussion

The lightcurves (Fig. 1) are fairly typical of cataclysmic variables in showing irregular flickering. However, oscillations at the X-ray period are not evident. In order to detect periodic signals hidden in noise, we calculated the amplitude spectrum for each observational night, using a fast Fourier transform (FFT) algorithm. Our lightcurves consist of about 3300 points. Since the FFT algorithm can operate only if lightcurves have a length of a power of 2, the lightcurves were padded with zeroes up to 4096 points. The corresponding amplitude spectra consist of

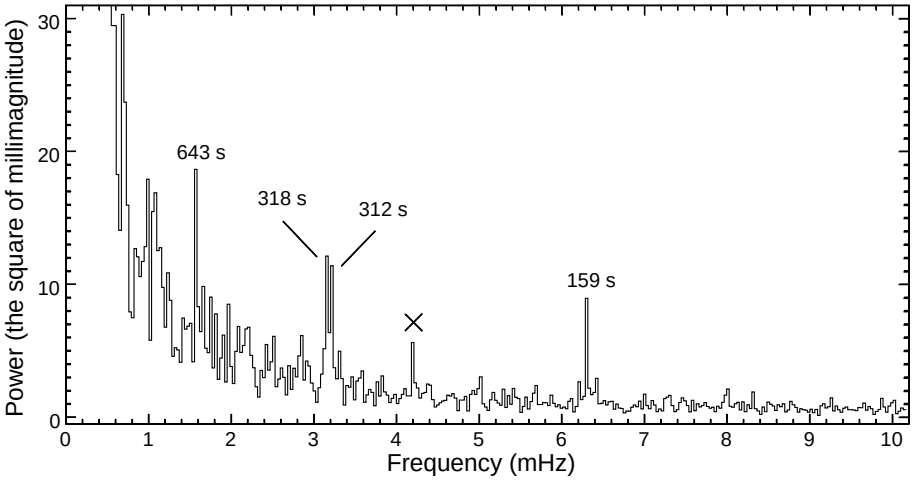

Fig. 3. Average power spectrum of V709 Cas with peaks labeled with their periods in seconds: 643, 318, 312, and 159. The peak marked with cross is an artifact caused by the telescope drive error which introduces a modulation with a period of 4 min

Table 2. Prominent peaks in the amplitude spectra

date (UT)	period (seconds)	semiampitude (mmag)
1999 Oct. 4	312.1 ± 1.4	6
1999 Oct. 4	159.1 ± 0.4	6
1999 Oct. 6	312.1 ± 1.4	8
1999 Oct. 7	643 ± 6	9
1999 Oct. 7	318.2 ± 1.5	5
1999 Oct. 8	643 ± 6	8
1999 Oct. 8	159.1 ± 0.4	5
1999 Oct. 9	318.2 ± 1.5	8
1999 Oct. 9	159.1 ± 0.4	6

2048 frequency components with frequency bins of 0.030517 mHz. These amplitude spectra are shown in Fig. 2. Three of them (October 4, 8 and 9) display the prominent peaks at a frequency of (6.287 ± 0.015) mHz. We consider the error equal to half the frequency bin. This frequency corresponds to a period of (159.1 ± 0.4) s. Within the accuracy of measurement this frequency agrees with the first harmonic of the orbital sideband if we specify a white dwarf rotation period of 312.78 s (Norton et al. 1999) and an orbital period of 5.4 h (Motch et al. 1996). The prominent peaks at a frequency of (3.143 ± 0.015) mHz are visible in the amplitude spectra on October 7 and 9. This frequency corresponds to a period of (318.2 ± 1.5) s. The amplitude spectra on October 4 and 6 display the prominent peaks at a frequency of (3.204 ± 0.015) mHz, which agree with the frequency of the X-ray pulsation. This frequency corresponds to a period of (312.1 ± 1.4) s. The prominent peaks at a frequency of (1.556 ± 0.015) mHz, which agree with the "subharmonic" of the orbital sideband, are visible in the amplitude spectra on October 7 and 8. This frequency corresponds to a period of (643 ± 6) s. The information about prominent peaks is given in Table 2.

In order to evaluate the statistical significance of detection of the observed oscillations, we calculated an average power spectrum since the prominent peaks in some of the amplitude spectra are often accompanied by the small peaks at the same frequencies in the other amplitude spectra. The amplitude spectra were squared and divided by $\sqrt{2}$. Then we took an average of these squared amplitude spectra. The average power spectrum is given in Fig. 3. The distinct peaks at frequencies corresponding to the X-ray period, the beat period and its first harmonic and subharmonic are easily visible in this power spectrum. Taking into account that each frequency component in an average power spectrum is distributed as $\chi^2(\nu)/\nu$, where ν is the number of degrees of freedom (see, for example, Bendat & Piersol 1986), we can find the probability that each of these peaks is a chance noise fluctuation. In our case the number of degrees of freedom, ν, equals 12 because of averaging of six power spectra.

The most significant peak in the average power spectrum corresponds to the first harmonic of the orbital sideband. The probability that this peak may be a chance noise fluctuation is less than 0.05%. Such a low probability shows that the detection of the oscillation at a period of 159 s is real beyond all manner of doubt. The statistical significance of detection of the oscillations at periods of 318 s and 312 s is somewhat worse. Each of the two peaks has a probability of 0.4% for a chance noise fluctuation. However, these two peaks agree with the subharmonic and its positive orbital sideband of the 159 s oscillation having the great statistical significance of detection, and therefore the detection of the 312 s and 318 s oscillations corresponding to the X-ray pulsation and its orbital sideband can be considered real also. The probability that the peak at a period of 643 s, which agrees with the subharmonic of the orbital sideband, may be a chance noise fluctuation is rather high, i.e. 1.3%. This peak lies within the region crowded with "noise" peaks due to flickering, and we cannot rule out the possibility that this peak could have arisen from noise fluctuations. In this case we have moderately high confidence (but not certainty) that the oscillation at a period of 643 s is real.

In order to evaluate more accurately the periods of the observed oscillations, we calculated an amplitude spectrum, using all the data sets together. For this purpose

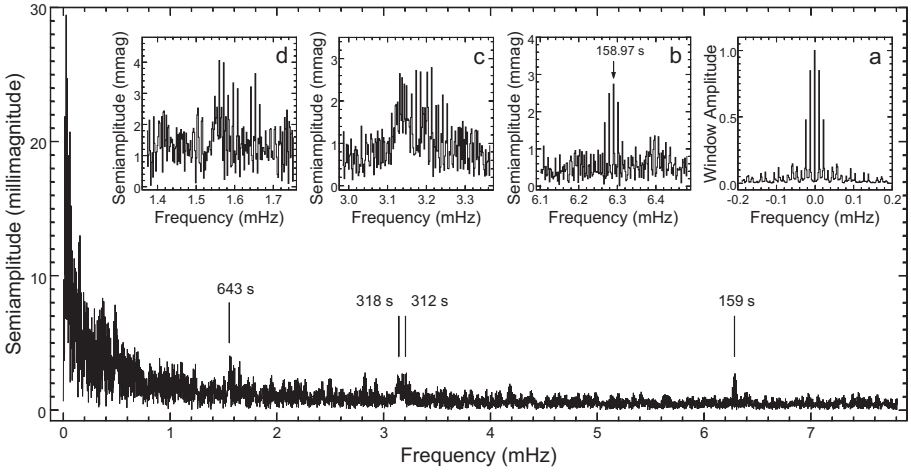

Fig. 4. Amplitude spectrum of V709 Cas calculated using all the data sets together. The inserted frame **a)** shows the window function. Vertical lines mark the frequencies at which the oscillations were detected using the average power spectrum. The inserted frames **b)**, **c)** and **d)** show the corresponding regions of large scale

we constructed a time series consisting of our lightcurves with the magnitudes averaged over 64 s time intervals and diurnal gaps padded with zeroes. A small deficiency of data at the end of the time series was also padded with zeroes. In order to prevent distortion of the amplitude spectrum due to abrupt change in the brightness of V709 Cas at the boundaries of the diurnal gaps, the nightly averages were removed from the lightcurves. As before, we calculated the amplitude spectrum, using the FFT algorithm. The amplitude spectrum presented in Fig. 4 consists of 4096 frequency components with frequency bins of 0.0019074 mHz. This amplitude spectrum clearly displays only the first harmonic of the orbital sideband. The corresponding peak (the inserted frame **b)**) has the distinct one-day aliases and a principal frequency of (6.2906 ± 0.0010) mHz, which corresponds to a period of (158.97 ± 0.03) s. Unfortunately, this amplitude spectrum cannot enable us to evaluate more accurately the periods corresponding to the X-ray pulsation, the orbital sideband and its subharmonic because the noise of these regions of the amplitude spectrum masks the signals (the inserted frames **c)** and **d)**).

One more method may be used in order to improve the significance of detection of the oscillations and evaluate more accurately their periods. This is classical one-way analysis of variance (AOV) (see, for example, Afifi & Azen 1979) in application to data folded and grouped into bins according to the phase of a trial period (Schwarzenberg-Szerny 1989). In this method the test statistic $\Theta_{\rm AOV}$ is defined as $\Theta_{\rm AOV} = s_1^2/s_2^2$, and the statistics s_1^2 and s_2^2 are defined as

$$(r-1)s_1^2 = \sum_{i=1}^{r} n_i(\bar{x}_i - \bar{x})^2\,, \qquad (1)$$

$$(n-r)s_2^2 = \sum_{i=1}^{r}\sum_{j=1}^{n_i}(x_{ij} - \bar{x}_i)^2\,, \qquad (2)$$

where $n, \bar{x}$ are the total number of observations and their average, r is the number of bins, $n_i, \bar{x}_i$ are the number of observations in the ith bin and their average and $x_{ij} = x(t_{ij})$ is the jth individual observation in the ith bin, obtained at time t_{ij}. An AOV periodogram, i.e. the test statistic $\Theta_{\rm AOV}$ as a function of the trial period P, may be used in order to search for periodic signals. Since the test statistic $\Theta_{\rm AOV}$ has F distribution with $r-1$ and $n-r$ degrees of freedom, the statistical significance of detection of periodic signals can be estimated.

However, statistically meaningful results from AOV periodograms may be derived if consecutive observations are uncorrelated. It is not the case in our observations of V709 Cas since the large amplitude flickering of this star renders the observations correlated. In order to solve this problem, we used filters that suppressed low frequencies in the observed lightcurves. The low frequencies were removed from the power spectra of the lightcurves. Then the filtered lightcurves were reconstructed, using an inverse Fourier transform algorithm. Since we took interest in certain intervals of periods of around 159 s, 312 s and 643 s, after numerical experiments we considered applicable to suppress the low frequencies up to 3 mHz, 1.5 mHz and 0.7 mHz for the analysis of each of these intervals of periods. Besides, the data in the lightcurves were averaged over 32 s, 64 s and 128 s time intervals in order to reduce the correlation length of the lightcurves additionally. The correlation length of each lightcurve was checked, using autocorrelation functions.

The AOV periodograms of V709 Cas are shown in Fig. 5. We used 5 bins per phase for each trial period. In all the cases the total number of the observations averaged over corresponding time intervals is more than 1000, and the critical value of the test statistic $\Theta_{\rm AOV}$ for the 0.1% significance level, which is shown in Fig. 5 as dashed lines, corresponds to $r-1=4$ and $n-r>120$ and equals 4.62. The AOV periodograms have a continuum level of about 1. This means that the consecutive observations are actually uncorrelated, and the results are statistically meaningful.

The most significant line in the AOV periodogram (Fig. 5a) corresponds to the first harmonic of the orbital sdeband. The one-day aliases can be easily differentiated from the principal line due to their low heights, and the period corresponding to the first

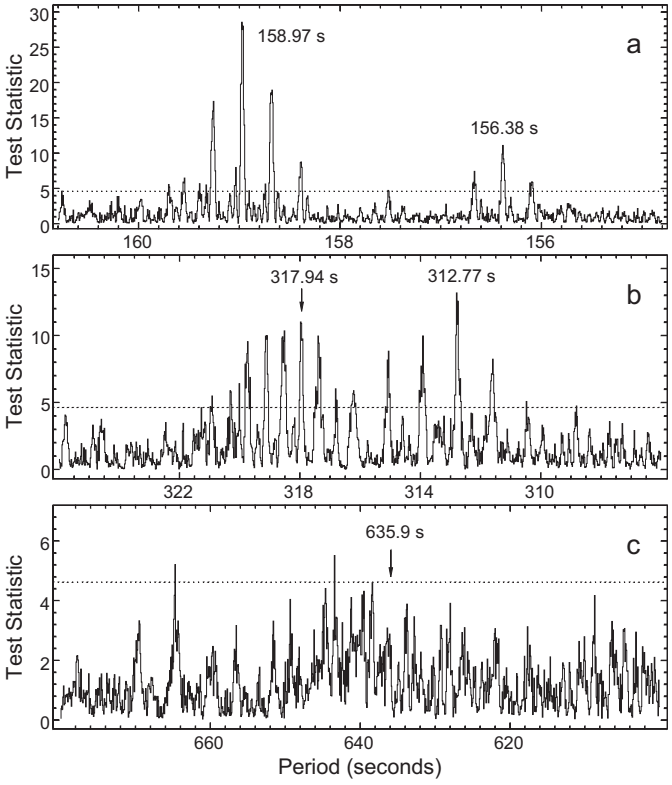

Fig. 5. AOV periodograms of V709 Cas. Trial periods cover the intervals in which the oscillations were detected using the average power spectrum. Each periodogram consists of 1000 points. The steps in trial periods equal 0.006 s in the frame **a)**, 0.02 s in the frame **b)** and 0.08 s in the frame **c)**. Dotted lines indicate the 0.1% significance level. Large lines are labeled with their periods in seconds. The arrow with a label of 635.9 s (the frame **c)**) marks the period corresponding to the subharmonic of the orbital sideband, which is absent in this periodogram

harmonic of the orbital sideband can be accurately evaluated. This period equals (158.97 ± 0.02) s. We consider the error equal to half the line width between half-intensity points. This AOV periodogram reveals one more period corresponding to the first harmonic of the X-ray pulsation. It equals (156.38 ± 0.02) s. The peaks corresponding to this period are also visible in the average power spectrum (Fig. 3) and the amplitude spectrum calculated using all the data sets together (the inserted frame **b)** of Fig. 4). Obviously, we cannot consider those peaks statistically significant since they exceed noise peaks in the power and amplitude spectra only slightly. Hence, AOV periodograms have better statistical properties and show the capability to detect weaker periodic signals in comparison with power spectra.

The AOV periodogram presented in Fig. 5b covers the intervals of periods, which enable us to analyze the oscillations corresponding to the X-ray period and the beat period. The largest line agrees with the X-ray period. In this case the one-day aliases can be easily differentiated. The principal line corresponds to a period of (312.77 ± 0.04) s, which is in agreement with the first harmonic of this oscillation. However, the structure of this periodogram in the vicinity of the beat period is rather unusual. Such a structure can be explained if we assume that the pulse profile of the sideband oscillation is "double-peaked". Then the coincidence of main pulses and satellite pulses in the folded lightcurves at some trial periods can produce additional lines between one- and two-day aliases, as well as between the principal line and one-day aliases, as seen in Fig. 5b. Besides, it is visible that the odd lines are wide and the even lines are sharp. This may mean that main pulses and satellite pulses are not separated by half the pulse cycle. It might be difficult to distinguish two large sharp lines (which of them is an one-day alias) because these lines have the nearly equal heights. However, as we know the period of the first harmonic of this oscillation, we must consider principal the line which corresponds to a period of (317.94 ± 0.04) s since this period is in agreement with the first harmonic of this oscillation.

Table 3. Finalized values of the detected periods

signal	period (seconds)
first harmonic of the spin frequency	156.38 ± 0.02
first harmonic of the orbital sideband	158.97 ± 0.02
spin period	312.77 ± 0.04
beat period	317.94 ± 0.04

The AOV periodogram presented in Fig. 5c does not reveal any statistically significant oscillations in the range 600–680 s. Moreover, the strict coincidence of the subharmonic of the orbital sideband (which is marked by the arrow) and any line is absent. Hence, the detection of the subharmonic of the orbital sideband in the average power spectrum (Fig. 3) is spurious. The increased continuum level in the range 638–646 s may be caused by temporary quasiperiodic oscillations which could also produce the peaks in the individual amplitude spectra on October 7 and 8 (Fig. 2). In Table 3 we give the finalized values of the detected periods.

Using radial velocities, Motch et al. (1996) evaluated the orbital period of V709 Cas equal to (5.4 ± 0.2) h or (4.45 ± 0.2) h, the two being one-day aliases of each other. In order to find out which of them is the actual orbital period, we attempted to recognize the corresponding peaks in the low-frequency part of the amplitude spectrum calculated using all the data sets together. This large-scale part of the amplitude spectrum is given in Fig. 6. While this part of the amplitude spectrum has no statistically significant peaks due to the high noise level, it displays two peaks corresponding to a periods of (5.20 ± 0.09) h and (4.28 ± 0.06) h, which are also one-day aliases of each other, and both peaks agree with the possible orbital periods within the accuracy of measurement. Unfortunately, this amplitude spectrum cannot give even a hint which of the two periods is the actual orbital period. However, using the accurately evaluated beat period, which equals (317.94 ± 0.04) s, we can easily set the range on possible orbital periods. If we will consider the spin period equal

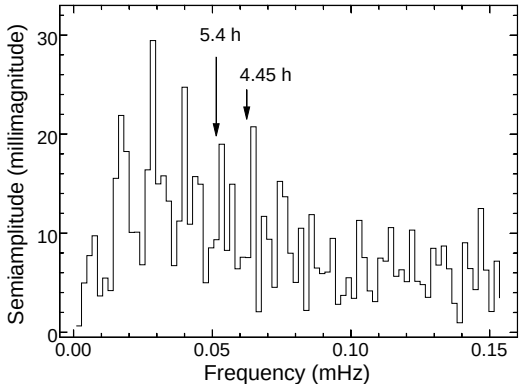

Fig. 6. Low-frequency part of the amplitude spectrum calculated using all the data sets together. Arrows with labels of 5.4 h and 4.45 h mark the possible orbital periods of V709 Cas (Motch et al. 1996). The largest peak corresponding to a period of (9.7 ± 0.3) h is not statistically significant

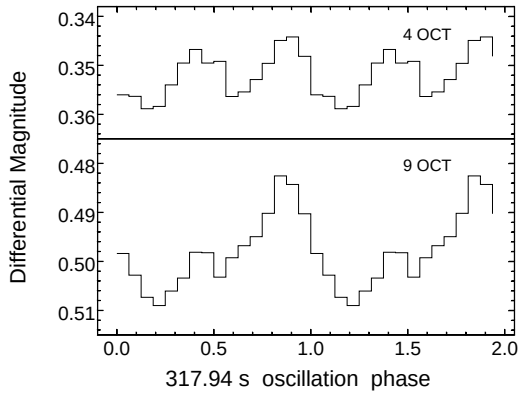

Fig. 7. The lightcurves of V709 Cas folded at a period of 317.8 s. 16 bins per phase are used and 83 oscillation cycles are averaged for each folded lightcurve. The pulse profile is double-peaked and variable from night to night

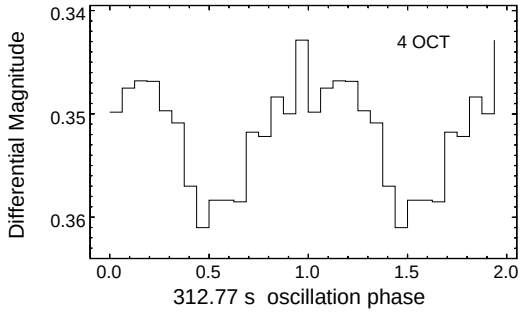

Fig. 8. The lightcurve of V709 Cas folded at a period of 312.77 s. 16 bins per phase are used and 85 oscillation cycles are averaged. The pulse profile is quasi-sinusoidal and cannot produce pronounced high-frequency harmonics

to (312.78 ± 0.03) s (Norton et al. 1999), then the orbital period must be in the range 5.28–5.43 h. If we will consider the spin period equal to (312.77 ± 0.04) s (present parer), then the orbital period must be in the range 5.26–5.43 h. Both results are very similar and show that the actual orbital period equals 5.4 h.

As mentioned, the complicated structure of the AOV periodogram in the vicinity of the beat period (Fig. 5b) can be explained if we assume that the pulse profile of the sideband oscillation is double-peaked. The presence of the strong first harmonic of the orbital sideband indicates also that the sideband oscillation is largely nonsinusoidal. In order to find the pulse profile of this oscillation, we folded the lightcurve obtained on October 9. The amplitude spectrum of this lightcurve displays the highest peak. The lightcurve folded at a period of 317.94 s is shown in the lower frame of Fig. 7. The pulse profile is double-peaked with two different maxima. This pulse profile must be variable from night to night since some of the amplitude spectra reveal only the first harmonic of this oscillation. Indeed, the upper frame of Fig. 7 shows the lightcuve folded at the same period, in which the maxima are nearly equal. This folded lightcurve corresponds to the observation on October 4, in which the amplitude spectrum reveals only the first harmonic of this oscillation. This amplitude spectrum displays one more prominent peak corresponding to the frequency of the X-ray pulsation. We folded this lightcurve at the X-ray period also. The pulse profile (Fig. 8) is quasi-sinusoidal.

The average power spectrum (Fig. 3) shows that the observed behaviour of oscillations in V709 Cas is rather unusual, i.e. the significant power occurs at the orbital sideband and its first harmonic while the fundamental does not show pronounced harmonics. Among known intermediate polars only Re 0751+14 shows similar behaviour of the orbital sideband (Hellier et al. 1994). It is believed that V709 Cas displays the double-peaked spin pulse profile in X-ray emission due to two-pole accretion, with most of the power at the fundamental, however (Norton et al. 1999). If the orbital sideband is caused by reprocessing of X-ray emission by the secondary star or the hot spot in the accretion disc, its optical pulse profile simply tracks the X-ray pulse profile and may be distorted due to asymmetry in reprocessing of X-rays from the two poles. This distorted pulse profile can produce the first harmonic in the optical power spectrum.

The quasi-sinusoidal pulse profile of the 312.77 s oscillation corresponding to the spin period of the white dwarf (Fig. 8) seems to be very interesting since the X-ray pulse profile of this star is double-peaked (Norton et al. 1999). This can be explained in "accretion curtain" model (Hellier 1995). In this model optical emission comes from the accretion curtains between the inner disc and the white dwarf. If they are optically thick, their varying aspect will produce a spin period modulation. Because the two poles of the white dwarf act in phase, the pulse profile may be quasi-sinusoidal. Norton et al. (1999) accounted for the double-peaked X-ray pulse profile of this star due to lower vertical optical depth (up the accretion curtain) in comparison with the horizontal optical depth (across it) to X-ray emission. In this case the two poles act in antiphase, and the pulse profile may be double-peaked.

4. Conclusions

1. We report detection of an optical counterpart of the 312.78 s X-ray pulse period of V709 Cas, its orbital sideband and the first harmonic of the orbital sideband;
2. The average semiamplitudes of all these signals are approximately equal to 0.005 mag;
3. A weak periodic signal corresponding to the first harmonic of the X-ray pulse period is also detected in the optical lightcurves of V709 Cas;
4. The pulse profile of the optical oscillation corresponding to the X-ray period is quasi-sinusoidal whereas the pulse profile of its orbital sideband is double-peaked and changes considerably from night to night;
5. The accurately evaluated beat period of V709 Cas enables us to set the range on possible orbital periods. The orbital period of V709 Cas must be in the range 5.28–5.43 h.

References

Afifi, A. A., & Azen, S. P. 1979, Statistical Analysis: a Computer Oriented Approax (Academic Press, New York–San Francisco–London)
Bendat, J. S., & Piersol, A. G. 1986, Random Data Analysis and Measurement Procedures (John Wiley & Sons, Ins.)
Haberl, F., & Motch, C. 1995, A&A, 297, L37
Hellier, C. 1995, in ASP Conf. Ser. 85, Proc. Cape Workshop on Magnetic CVs, ed. D. A. H. Buckley, & B. Warner, Astron. Soc. Pas., San Francisco, 185
Hellier, C., Ramseuer, T. F., & Jablonski, F. J. 1994, MNRAS, 271, L25
Kozhevnikov, V. P., & Zakharova, P. E. 2000, in ASP Conf. Ser. 219, Proc. Euroconference on Disks, Planetesimals and Planets, ed. F. Garzon, & T. J. Mahoney, in press
Motch, C., Haberl, F., Guilliot, P., et al. 1996, A&A, 307, 459
Norton, A. J., Beardmore, A. P., Allan, A., & Hellier, C. 1999, A&A, 347, 203
Patterson, J. 1994, PASP, 106, 209
Schwarzenberg-Czerny, A. 1989, MNRAS, 241, 153